Modulated optical solid-state spectrometer applications in plasma diagnostics

John Howard
Plasma Research Laboratory, Australian National University, Canberra ACT 0200, Australia

(Presented on 8 June 1998)

A new electro-optically modulated optical solid-state (MOSS) interferometer has been constructed for the measurement of the low order spectral moments of line emission from optically thin radiant media. The instrument, which is based on the principle of the Fourier transform spectrometer, is rugged, compact, and inexpensive and offers a number of advantages over conventional grating based spectrometers. Most importantly, by employing electro-optical path-length modulation techniques, the spectral information is obtained using a single photomultiplier tube. Specifically, the zeroth moment (brightness) is given by the average signal level, the first moment (shift) by the modulation phase and the second moment (line width) by the modulation amplitude. In applications such as Zeeman spectroscopy and motional Stark effect (MSE), polarization modulation can be used to effect a modulation of the center frequency and/or coherence of the light which is then measured by the MOSS spectrometer. This article describes a number of applications, including Doppler and charge exchange recombination spectroscopy and polarization spectroscopy (Zeeman and MSE) for which the MOSS spectrometer is an inexpensive and powerful alternative to multichannel grating spectrometers. © *1999 American Institute of Physics.* [S0034-6748(99)74601-0]

I. INTRODUCTION

This article describes an electro-optically modulated solid state (MOSS) spectrometer for general purpose optical plasma spectroscopy.[1,2] The spectrometer monitors the temporal coherence and center of mass of an isolated spectral line using polarization interferometric techniques. It is essentially a Fourier transform spectrometer modulated about a fixed delay. The amplitude of the interference fringes produced by the modulation is related to the light temporal coherence while the phase conveys the line center frequency.

The MOSS spectrometer is shown in Fig. 1. A narrowband interference filter isolates the spectral line of interest. The first polarizing cube transmits the horizontally polarized component of the filtered plasma light to a birefringent crystal (typically $LiNbO_3$, $L=25$ mm thick, birefringence $B=0.1$) whose fast axis is at 45° to the plane of polarization. For light of center frequency $\nu_0=c/\lambda_0$, this introduces a phase delay $\phi_0=2\pi\nu_0 BL/c=2\pi\nu_0\tau_0$ between the orthogonal characteristic waves. An additional small delay modulation $\tilde{\phi}_1=2\pi\nu_0\tilde{\tau}_1=\phi_1\sin(\Omega t)$ of amplitude $\phi_1=\pi/2$ is imposed by applying an oscillating voltage (typically at tens of kilohertz) along the crystal z axis. Finally, the light is once more polarized using a beam splitter cube to allow the independent components to interfere at photomultiplier tubes intercepting the transmitted and reflected beams. Because of the large fixed delay τ_0, small changes in wavelength can give significant shifts in the interferogram phase that manifest as a change in the ratio of fundamental and second-harmonic modulation components.

The intensity at the output port is proportional to

$$S_{\pm}=\int_0^{\infty} g(p,\hat{\mathbf{l}};\nu)[1\pm\cos(2\pi\nu\tau)]d\nu, \tag{1}$$

where $\tau=\tau_0+\tilde{\tau}_1$ is the total time delay introduced by the birefringent crystal and $g(p,\hat{\mathbf{l}};\nu)$ is the line integrated intensity at impact parameter p and in the direction $\hat{\mathbf{l}}$. Issues of sensitivity and resolution are discussed at length elsewhere.[2]

II. DOPPLER SPECTROSCOPY

The most basic optical spectroscopy measures the Doppler shift and broadening of emission from excited plasma atoms and ions. Usually these measurements are line integrated, though charge exchange recombination spectroscopy achieves a degree of localization. For concreteness, we assume a locally Maxwellian, isotropic emission profile:

$$I(\mathbf{r},\hat{\mathbf{l}};\nu)=\frac{I_0(\mathbf{r})}{\sqrt{2\pi}\sigma(\mathbf{r})}\exp\left[-\frac{(w-\beta_D)^2}{2\sigma^2(\mathbf{r})}\right], \tag{2}$$

where $\mathbf{r}$ is a position in the plasma, and $I_0(\mathbf{r})$ is the local emission intensity. Here $w=(\nu-\nu_0)/\nu_0$ is a normalized frequency coordinate, ν_0 is the emission line center frequency and $\beta_D=\boldsymbol{\beta}_D(\mathbf{r})\cdot\hat{\mathbf{l}}$ with $\boldsymbol{\beta}_D(\mathbf{r})=\mathbf{v}_D(\mathbf{r})/c$, where $\mathbf{v}_D$ is the bulk flow velocity of the emitting species. The species temperature is given by $kT_s(\mathbf{r})/(m_s c^2)=\sigma^2(\mathbf{r})$, where m_s is the atomic weight.

It has been shown that the three lowest order spectral moments of the line-integrated emission can be related by a Radon transform to the corresponding velocity moments of the ion or atom velocity distribution function.[3] For brevity, however, we ignore the spatial integration and combine Eqs. (1) and (2) to obtain a quantity proportional to the signal at the spectrometer ports

$$S_{\pm}=I_0\pm I_0\zeta\cos[\phi_0(1+\beta_D)+\phi_1\sin(\Omega t)], \tag{3}$$

where the fringe visibility

$$\zeta_S=\exp[-T_S/T_C] \tag{4}$$

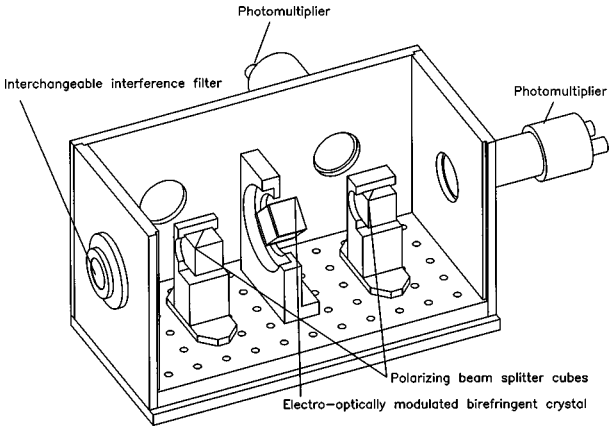

FIG. 1. Optical layout for the modulated solid state spectrometer.

depends on the species temperature T_S and

$$kT_C = \tfrac{1}{2} m_S v_C^2, \tag{5}$$

$$v_C = \frac{2c}{\phi_0}. \tag{6}$$

T_C is a ''characteristic temperature'' set by the phase delay introduced by the birefringent crystal and v_C is the corresponding ''characteristic velocity.'' We have ignored terms of order ϕ_1/ϕ_0 in the expression for T_C. Observe that the small Doppler shift component is amplified by the fixed phase delay ϕ_0.

The unknown quantities I_0, β_D, and T_S can be recovered numerically from $S_\pm$ synchronously sampled at times $t = 0, T/4, T/2, 3T/4, \ldots$, where $T = 2\pi/\Omega$ is the modulation period. In practice, the maximum fringe contrast is set by instrumental factors, the collected light solid angle and nonideal optical components, and can be accounted by introducing the factor $\zeta_I = \exp(-T_I/T_C)$, where T_I is the instrument ''temperature.'' Because this is a ''time-domain'' instrument, the instrument response can be compensated through a simple subtraction of exponents proportional to the measured and instrumental temperatures rather than the usual deconvolution procedure.

To illustrate the instrument performance, we present here temperature and flow data for an rf heated (7 MHz, 80 kW max) argon discharge in a low-shear magnetic configuration close to the 3/2 resonance in the H-1NF helical axis stellarator at the ANU.[4] Under these conditions, transitions from low to high confinement are achievable at low magnetic field strengths ($\sim 0.1T$) and low heating power.[5] Ar II light at 488 nm is collected from a cylindrical plasma volume of diameter ~ 30 mm with axis parallel to the major axis of the bean-shaped plasma cross section. The viewing cylinder can be translated across the plasma poloidal cross section on a shot-to-shot basis.

The observed ion temperatures for these conditions are in the range 10–100 eV and match well the dynamic range for a $LiNbO_3$ crystal of thickness 25 mm ($T_C = 70$ eV). The instrument temperature, measured using an expanded argon ion laser beam at 488 nm is ~ 20–25 eV and arises from imperfections in the birefringent plate. The estimated component due to beam divergence is less than a few eV. The sensitivity to temperature and flow speed changes clearly depends on the light signal to noise ratio.

Figure 2 shows the temporal evolution of various diagnostic signals for a discharge that exhibits a spontaneous transition from low to high confinement at $t = 15$ ms. The top two traces are the plasma line averaged density and stored energy measured using a 2 mm quadrature interferometer and magnetic flux loop, respectively. The MOSS quadrature sampled signal (4×42 kHz) for a chord at impact parameter $p = 20$ mm outside the plasma axis is the third trace. The ratio of the maximum separation of the four traces to their mean value gives the fringe visibility or contrast. The contrast, as noted above, depends on the ion temperature. A five-point running mean has been applied to the light-related signals. The following three traces are the inferred zeroth moment $\langle I_0 \rangle$, ion temperature $\langle T_S \rangle$, and flow velocity $\langle \beta_D \rangle$, where angle brackets denote line-averaged quantities. The last trace shows the Ar I light intensity at 763.5 nm. The noise levels for the ion temperature and flow are consistent with estimates based on the light signal-to-noise ratio. Observe the decrease in fringe contrast following the transition, indicating an increase in the ion temperature. The instrument temperature has not been subtracted from the temperatures displayed here. Also note that the change in flow velocity throughout the transition is only of order 500 m/s. This is also true at other impact parameters. These results are consistent with electric probe measurements showing that the ion pressure balance after the transition is maintained by a decrease in the central electric potential, with the role of flows being minimal.

By virtue of its high light throughput (in our case, ~ 40 times greater than for an equivalent-resolution grating instrument) and direct sensitivity to low order spectral moments, the MOSS spectrometer is especially well suited to the measurements that require high time resolution such as for the observation of fluctuations and coherent modes. Figure 3 shows diagnostic signals during rf power modulation experiments on H-1NF. Observe the similarity in temporal behavior of the plasma stored energy (trace 3) and the ion temperature (bottom trace). Also note the (somewhat noisy) associated variation in the plasma flow velocity. The light-related signals have been subjected to a 20-point running mean while the viewing chord impact parameter was 0 mm in this case (i.e., the chord intercepts the plasma axis).

III. POLARIZATION SPECTROSCOPY

The presence of a magnetic or electric field removes the degeneracy of transition energy levels, resulting in the familiar Zeeman and Stark split multiplets. The multiplet components have polarization states that depend on the change in magnetic quantum number ΔM, the orientation of the field and the direction of view. By filtering the polarization state of the collected light, we can vary either its coherence (bandwidth) or its center of mass (or both). Since the MOSS spectrometer is sensitive to both quantities, this is a potentially powerful method for detecting both the strength and orientation of plasma electric and magnetic fields.

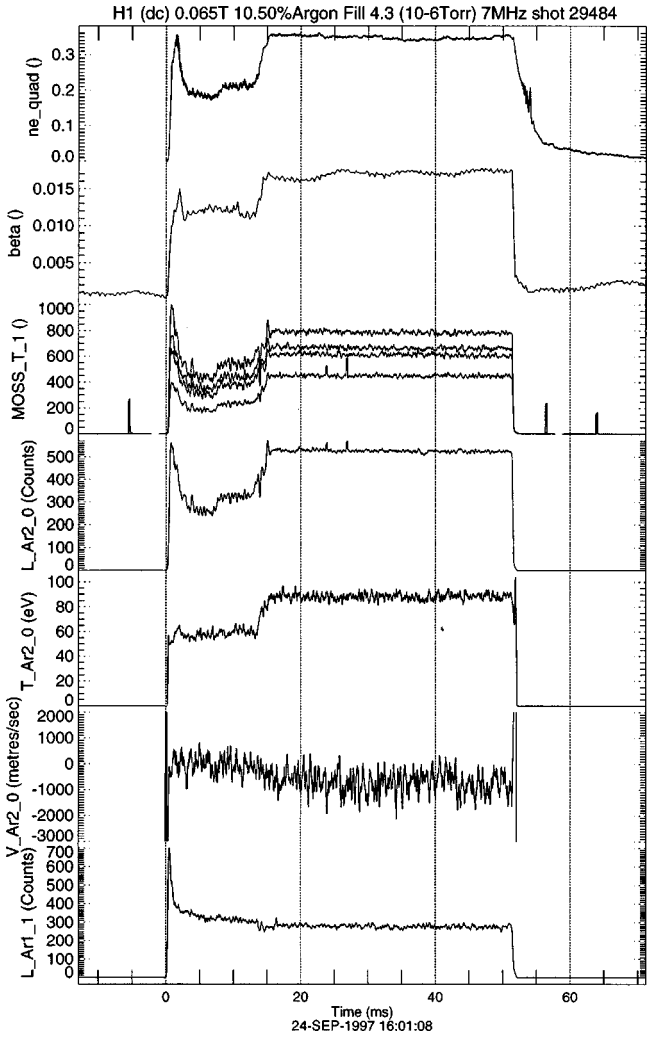

FIG. 2. Plasma parameters during spontaneous transition from low to high confinement at $t=15$ ms. Top to bottom: Plasma stored energy, line-averaged density, quadrature sampled MOSS light signal at impact parameter $+20$ mm, light intensity, inferred temperature, flow velocity, and atom light intensity. Note the small decrease in atom light emission and slight deviation in flow velocity at the time of the transition. The dc offset for the flow speed is not significant.

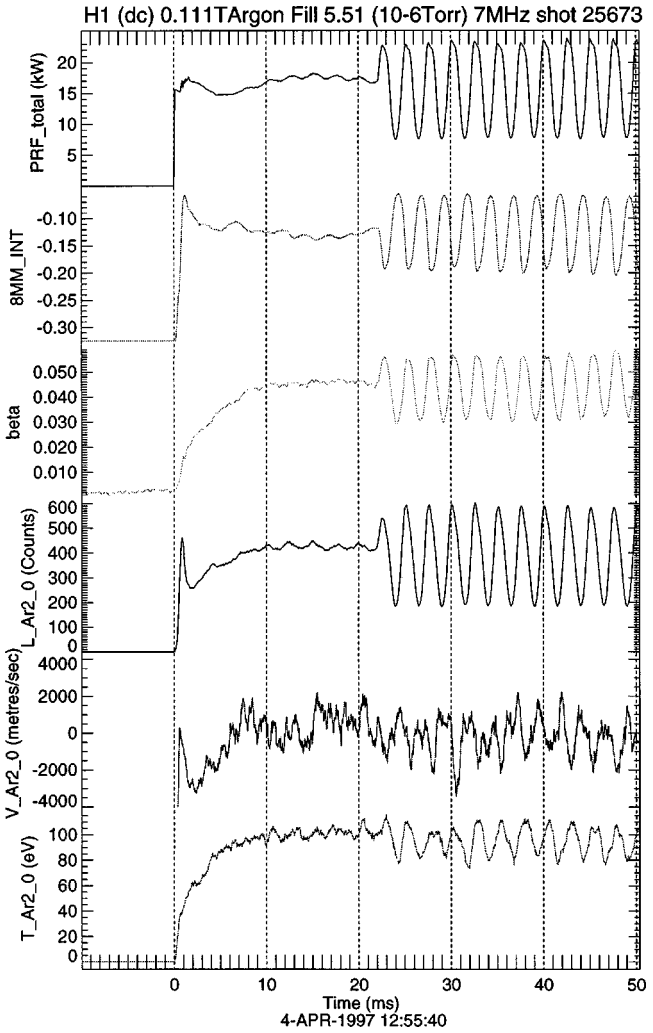

FIG. 3. Diagnostic signals during low power rf modulation experiments. From top to bottom, the signals are the rf power to the plasma, 8 mm homodyne interferometer signal, the plasma stored energy, the MOSS light intensity, flow velocity and ion temperature. Note the close correspondence between the temporal behavior of the stored energy and the ion temperature.

A. Polarimeter

The polarimeter uses two birefringent phase plates (delays δ_1 and δ_2) having their fast axes mutually oriented at 45°. The plates are followed by an analyzer oriented to transmit light polarized parallel to the fast axis of the first phase plate (the x direction) (Fig. 4). The intensity of the light transmitted (or reflected) by the analyzer is related to the Stokes vector of the input radiation by[6]

$$P=\frac{I_0}{2}(1\pm\mathbf{s}\cdot\mathbf{p}), \tag{7}$$

$$\mathbf{s}=(\cos 2\psi\cos 2\epsilon,\sin 2\psi\cos 2\epsilon,\sin 2\epsilon), \tag{8}$$

$$\mathbf{p}=(\cos\delta_2,\sin\delta_2\sin\delta_1,\sin\delta_2\cos\delta_1), \tag{9}$$

where $\mathbf{s}$ is the Stokes vector and ψ and ϵ are the tilt angle with respect to the x axis and the ellipticity of the vibrational ellipse, respectively. Equations (8) and (9) represent points on the Poincaré sphere. Accordingly, it is clear that if the phase plates are replaced by photoelastic modulators[7] operating at frequencies Ω_1 and Ω_2, it is possible, using appropriate delay amplitudes and synchronous detection techniques to measure simultaneously all the components of $\mathbf{s}$.

B. Zeeman effect

In the presence of B, a spectral line can be split into a number of components whose relative intensities and polarizations depend on the corresponding changes in the total angular momentum and magnetic quantum numbers J and M.[8] Viewed in the direction of B, the intensity is zero for the $\Delta M=0$ or π lines and is circularly polarized clockwise for $\Delta M=+1$ and counterclockwise for $\Delta M=-1$. The frequency shift for the circularly polarized or σ components depends linearly on B and is independent of the transition frequency. For fusion devices, the transition splitting is generally small compared to the Doppler broadening. Polarization filtering of the frequency shifted Zeeman components is

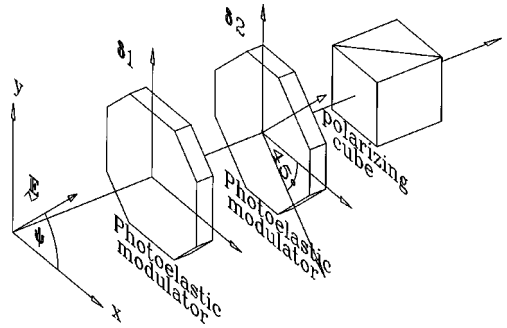

FIG. 4. Layout of spherical quadrature polarimeter based on variable phase delay birefringent plates and analyzer.

thus essential for their discrimination against the thermally broadened component.

The spectrum and polarization state of the emergent radiation is the integral over the line of sight of the intensity weighted contributions from the circular and linear components. For plate delays $\delta_1 = 0$ and $\delta_2 = \pi/2 \sin \Omega t$, the polarimeter signal alternately registers only the right and left circularly polarized components, with weight proportional to $\cos \gamma$ where γ is the angle between the line of sight and **B**. The wavelength separation gives rise to an associated modulation in the center wavelength of the transmitted radiation entirely analogous to the Doppler shift discussed above. The total first spectral moment is now given by[3]

$$\mu^{(1)} = \mu_D^{(1)} + \mu_B^{(1)} \sin \delta_2, \tag{10}$$

where $\mu_B^{(1)}$ gives the intensity weighted component of the poloidal magnetic field integrated along the line of sight:

$$\mu_D^{(1)} = \int_0^L I_0(\mathbf{r}) \boldsymbol{\beta}_D \cdot d\mathbf{l}, \tag{11}$$

$$\mu_B^{(1)} = \int_0^L I_0(\mathbf{r}) \boldsymbol{\beta}_B \cdot d\mathbf{l}. \tag{12}$$

Here

$$\beta_B = \frac{g \mu_B}{h \nu_0} \mathbf{B}(\mathbf{r}),$$

where μ_B is the Bohr magneton and g a constant of order unity.

As for Doppler measurements, this is a longitudinal vector tomography problem. From sufficient measurements can be recovered the divergence-free component of the vector field $I_0\mathbf{B}$. When the emission is constant on a flux surface, the magnetic field itself can be unambiguously recovered.

C. Motional Stark effect

Motional Stark effect (MSE) polarimetry is now a standard diagnostic for estimating magnetic field pitch angle in tokamaks using high power heating beams.[9–12] The MSE technique relies on the splitting of the high energy neutral beam Balmer α light into orthogonally polarized σ and π components as a result of the motion-induced strong electric field $\mathbf{E} = \mathbf{v} \times \mathbf{B}$ experienced in the rest frame of the neutral atoms. When viewed in a direction perpendicular to **E**, the

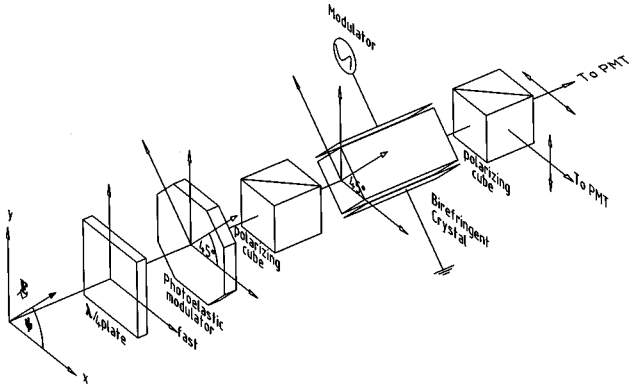

FIG. 5. Schematic diagram of the combined polarimeter and MOSS spectrometer arrangement necessary for contrast modulation MSE measurements.

Stark split σ and π components are polarized respectively perpendicular and parallel to the direction of **E**. When viewed along **E** the σ components are unpolarized and the π components have no intensity. The magnetic field pitch angle is usually estimated by isolating and measuring the polarization direction of the central cluster of σ lines. However, extension of the technique to boot-strap current driven low field compact devices is problematic because Doppler broadening due to heating beam divergence masks the separation of the σ and π components.

In combination with the above-described polarimeter, the MOSS senses the variations in the coherence of the orthogonally polarized σ and π components transmitted alternately by the polarimeter (see Fig. 5). This is a complementary approach to the frequency domain narrowband filters usually applied to isolate the central σ components. The new method, which has been discussed at length elsewhere,[13] potentially increases the useful operating parameter range for the MSE diagnostic.

ACKNOWLEDGMENT

It is a pleasure to acknowledge technical assistance provided by Mr. Rob Davies.

[1] Australian Scientific Instruments A Division of Anutech Pty Ltd, phone: 61 2 6280 7570, Fax: 61 2 6280 4985. Contact John Hyder@asi.anutech.com.au
[2] J. Howard, Rev. Sci. Instrum. (to be published).
[3] J. Howard, Plasma Phys. Controlled Fusion **38**, 489 (1996).
[4] S. M. Hamberger, B. D. Blackwell, L. E. Sharp, and D. B. Shenton, Fusion Technol. **17**, 123 (1990).
[5] M. Shats *et al.*, Phys. Rev. Lett. **77**, 4190 (1996).
[6] J. Howard, Rev. Sci. Instrum. **66**, 383 (1995).
[7] Hinds Instruments, 3175 NW Aloclek Drive, Hillsboro, OR 97124-7135.
[8] U. Feldman *et al.*, J. Appl. Phys. **56**, 2512 (1984).
[9] F. M. Levinton *et al.*, Phys. Rev. Lett. **63**, 2060 (1989).
[10] F. M. Levinton *et al.*, Rev. Sci. Instrum. **61**, 2914 (1990).
[11] D. Wroblewski *et al.*, Rev. Sci. Instrum. **61**, 3552 (1990).
[12] D. Wroblewski and L. L. Lao, Rev. Sci. Instrum. **63**, 5140 (1992).
[13] J. Howard, Plasma Phys. Controlled Fusion (to be published).